*Journal of Applied Mechanics and Technical Physics, Vol. 39, No. 3, 1998*

# DECAY OF A CENTERED PRANDTL–MAYER COMPRESSION WAVE IN A STEADY GAS FLOW

A. V. Omel'chenko and V. N. Uskov

UDC 533.6.011.72

*Discontinuity decay at a singular point of a centered compression wave is considered. Analytical solutions are given that allow one to determine the type of reflected discontinuity that issues from the point of decay and the boundaries of ranges of parameters within which a solution of the problem exists.*

**Introduction.** The problem of decay of an arbitrary stationary discontinuity in a plane homogeneous supersonic flow of an ideal inviscid gas is a traditional problem of supersonic gas dynamics. This problem, formulated for the first time by Landau [1], still attracts the attention of researches [2–5].

In the present paper, we consider a particular case of the problem — discontinuity decay at a singular point of a centered compression wave. From analysis of isomachs in the plane of wave intensities, Adrianov et al. [4], and Omel'chenko and Uskov [6] obtained analytical solutions that allow one to determine the type of reflected discontinuity that issues from the point of decay, the boundaries of ranges of the initial parameters within which a solution of the problem exists, and optimal waves for various parameters of the problem [6].

The solutions obtained are of both theoretical and applied significance and can be used in the gas-dynamic design of supersonic air intakes, facilities of jet technology, and other equipment.

**1.** We consider a Prandtl–Meyer centered compression wave (Fig. 1) in an ideal gas flow at known Mach number M and adiabatic exponent $\gamma$. The ratio of the static pressures behind the wave $p_1$ and ahead of the wave $p$ are treated as the intensity $J_1$ ($J_1 = p_1/p$) of wave 1. The modulus of the flow deflection angle in a simple wave is determined using the known Prandtl–Mayer functions:

$$\beta_1(\mathrm{M}, J) = |\omega(\mathrm{M}_1) - \omega(\mathrm{M})|. \tag{1.1}$$

The relationship of the Mach numbers ahead of the wave M and behind the wave $\mathrm{M}_1$ is established using the following general relation for isentropic $i$ and shock $j$ waves [6]:

$$\mu/\mu_1 = J/E \quad [\mu = 1 + \varepsilon(\mathrm{M}^2 - 1), \quad E = \rho/\rho_1, \quad \varepsilon = (\gamma - 1)/(\gamma + 1)]. \tag{1.2}$$

The values of $E$ and $J$ are related by the Rankine–Hugoniot adiabat for $j$ waves and the Laplace–Poisson adiabat for $i$ waves:

$$E^{(j)} = (J + \varepsilon)/(1 + \varepsilon J), \qquad E^{(i)} = J^{1/\gamma}. \tag{1.3}$$

Hence, the value of $\mathrm{M}_1$ in (1.1) is determined with allowance for (1.2) and (1.3) from the formula

$$\mu_1 = \mu J^{-1/\eta} \qquad [\eta = (1 + \varepsilon)/2\varepsilon]. \tag{1.4}$$

The condition $\mathrm{M}_1 \geqslant 1$ restricts values of the compression-wave intensity and flow-deflection angle to the quantities $J_*$ and $\beta_*$, which are calculated by the formulas

$$J_*(\mathrm{M}) = \mu^{\eta}, \qquad \beta_*(\mathrm{M}) = \omega(\mathrm{M}). \tag{1.5}$$

Baltiisk State Technical University, St. Petersburg 198005. Translated from Prikladnaya Mekhanika i Tekhnicheskaya Fizika, Vol. 39, No. 3, pp. 59–68, May–June, 1998. Original article submitted 27 September, 1996.

0021-8944/98/3903-0375 $20.00  

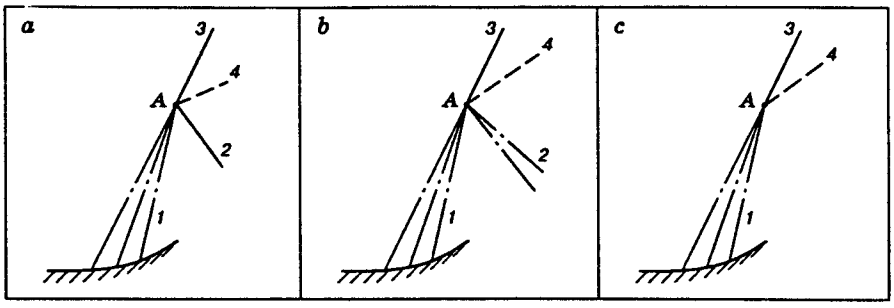


Fig. 1

The center of the compression wave (point A in Fig. 1) is a singular point at which wave decay occurs [1]. The decay is accompanied by formation of reflected decay 2 and the resulting shock 3, which issue from point A and have different directions. In Fig.1, the directions of the main (resulting) shock 3 and the compression wave 1 coincide, and, hence, they have identical indices of direction $\chi_i$ ($\chi_1 = \chi_3 = +1$) [4]. The reflected discontinuity is oppositely directed ($\chi_2 = -1$) and can be both a shock [$\lambda_2^{(j)} = \operatorname{sign}\Lambda = +1$, $\Lambda = \ln J$] (Fig. 1a) and a centered rarefaction wave [$\lambda_2^{(i)} = -1$] (Fig. 1b). In a particular case, the reflected discontinuity can be absent (wave decay without reflection) (Fig. 1c).

The problem of discontinuity decay is formulated as follows: for a flow with known M and $\gamma$ it is required to determine the intensities of the discontinuities that issue from the point A from a given intensity $J_1$ of the centered compression wave. The solution is constructed on the basis of the traditional conditions of dynamic compatibility for the tangential discontinuity 4, which issues from the point A. These conditions lead to a system of equations (a system for the decay) for the intensity $J_3$ of the strong shock 3 and for the intensity $J_2$ of the reflected discontinuity 2:

$$J_1 J_2 = J_3; \tag{1.6}$$

$$\beta_1(\mathrm{M}, J_1) + \psi_2\beta_2(\mathrm{M}_1, J_2) = \beta_3(\mathrm{M}, J_3). \tag{1.7}$$

The index of the flow deflection angle is $\psi = 1$ if the flow past the wave rotates counterclockwise, and it is $\psi = -1$ in the opposite case. The positive and negative values of the quantities $\psi$, $\lambda$, and $\chi$ are related by the simple relation [4]

$$\psi = \lambda\chi. \tag{1.8}$$

Hence, $\psi_1 = \psi_3 = 1$, and $\psi_2^i = 1$ for the reflected rarefaction wave (Fig. 1b), and $\psi_2^j = -1$ for the shock (Fig. 1a).

The modulus of the deflection angle $\beta_2$ for the reflected rarefaction wave is calculated from formula (1.1) using the Mach numbers behind the compression wave $\mathrm{M}_1$ and behind the reflected wave $\mathrm{M}_2$. The value of $\mathrm{M}_2$ is expressed in terms of $J_2$ by formula (1.4) with corresponding replacement of the index.

If the reflected discontinuity is a shock, the angle $\beta_2$ is obtained from the relation

$$\beta(\mathrm{M}, J) = \arctan\left[\sqrt{\frac{J_m - J}{J + \varepsilon}}\,\frac{(1-\varepsilon)(J-1)}{J_m + \varepsilon - (1-\varepsilon)(J-1)}\right] \qquad [J_m = (1+\varepsilon)\mathrm{M}^2 - \varepsilon] \tag{1.9}$$

using $\mathrm{M}_1$ and $J = J_2$. In this case, $\mathrm{M}_1$ is expressed in terms of the parameters M and $J_1$ from (1.2) with allowance for the first formula of (1.3).

In addition, the deflection angle $\beta_3$ on the resulting shock 3 can be calculated by relation (1.9) from the given values of M and $J = J_3$.

The problem is to determine the boundaries of ranges of the initial parameters (M, $J_1$, and $\gamma$) within which reflected discontinuities of various types occur, the boundaries of ranges in which the formulated problem does not have solutions, and the intensities of optimal waves [6].

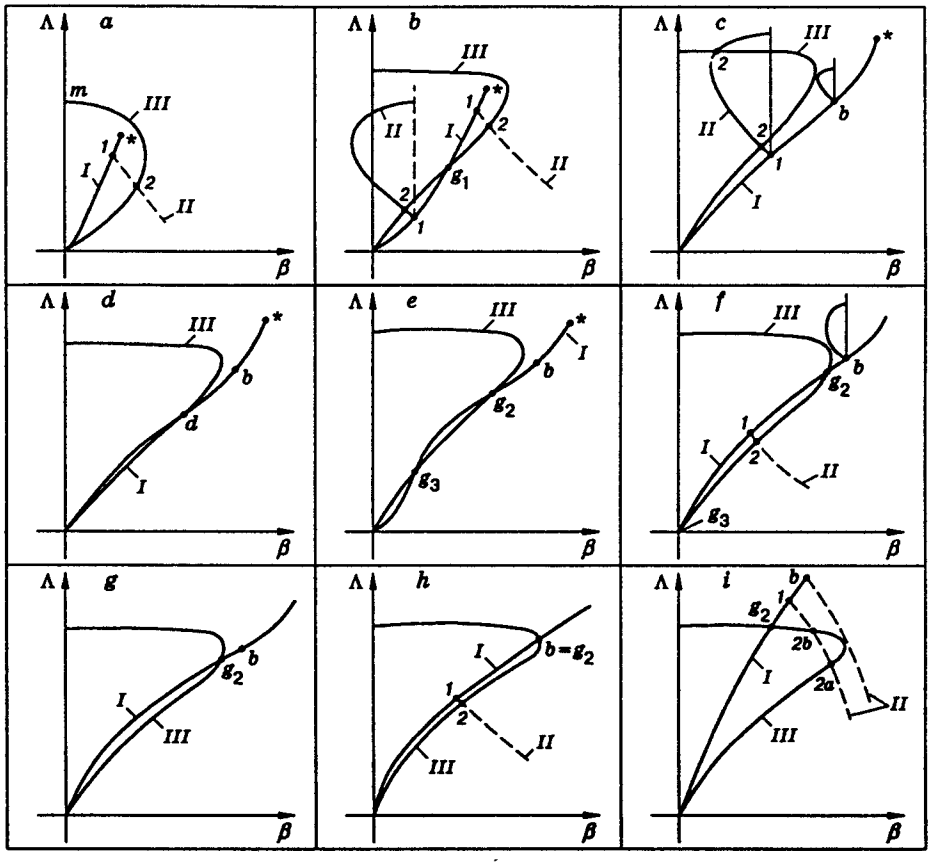


Fig. 2

2. Analysis of the solution of the decay system (1.6) and (1.7) is conveniently performed on the plane of the wave intensities ($\Lambda = \ln J$, $\beta$) [4, 6] (Fig. 2). The curves of constant Mach numbers (isomachs) on this plane are constructed on the basis of relations (1.1), (1.4), and (1.9). The isomach of a shock is usually called a heart-shaped curve. In Fig. 2, curves I–III are the isomachs of the compression wave and the reflected and main shocks, respectively. Points 1 on the isomach I correspond to the specified value of $J_1$ and have coordinates $\Lambda_1$ and $\beta_1$. The dashed curves II in Fig. 2 show the reflected discontinuities 2 (see Fig. 1). According to formula (1.8), these curves are either the right branch of the rarefaction wave or the left branch of the heart-shaped curve. They are constructed in a coordinate system with origin at point 1 on the isomach I (Fig. 2) and are described by formulas (1.1) and (1.4) in which the subscript 1 is replaced by the subscript 2, and M is replaced by $M_1$ in the first case or by formula (1.9) for $M = M_1$ and $J = J_2$ in the second case.

Point 2 (Fig. 2) of intersection of curves II and III is a graphical solution of system (1.6) and (1.7). Its coordinates on the heart-shaped curve III give the intensity $J_3$ of the main shock and the flow deflection angle $\beta_3$ at this shock. The coordinates $\Lambda_2$ and $\beta_2$ in the coordinate system with origin at point 1 correspond to the same characteristics of the reflected discontinuity.

Figure 2 gives possible solutions of the problem for various values of the initial parameters M and $J_1$ and a constant value of $\gamma$. Figure 2a refers to the solution with a reflected rarefaction wave, and point 2 in Fig. 2b refers to a reflected shock. The points $g_i$ of intersection of isomachs I and III in Fig. 2b and e–i illustrate compression-wave decay without a reflected discontinuity ($J_2 = 1$ and $\beta_2 = 0$).

Qualitative analysis of Fig. 2 shows that the solution depends on the position of point 1 relative to curve III. In the case of a weak compression wave, the relative position of the isentropic curves I and the heart-shaped curves III is determined by the values of the derivatives $\partial^k \Lambda / \partial \beta^k$ of the $k$th order at the coordinate origin, obtained using relations (1.1), (1.4), and (1.9) in which $J_3 \to 1$ and $J_1 \to 1$. Analysis of

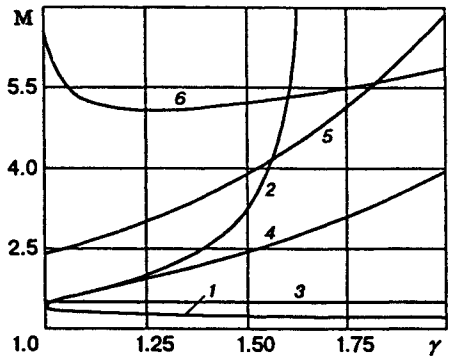


Fig. 3

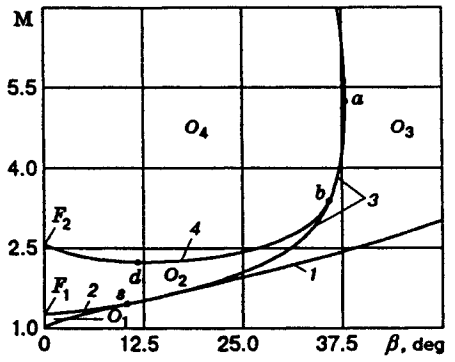


Fig. 4

these derivatives shows that curves I and III at the coordinate origin have second-order tangency for any M, and for

$$M_{F_i} = \sqrt{\frac{2}{5-3\gamma}\left[(3-\gamma)\mp\sqrt{\gamma^2-1}\right]} \qquad (i=1,\,2), \tag{2.1}$$

their third-order derivatives also coincide. In this case, in the range $M \in [1, M_{F_1}] \cup [M_{F_2}, \infty)$, we have $\partial^3\Lambda_3/\partial\beta_3^3 < \partial^3\Lambda_1/\partial\beta_1^3$, and in the range $M \in [M_{F_1}, M_{F_2}]$, the inverse inequality is valid. This means that in the first case, the decay of a weak compression wave ($J_1 \approx 1$) is accompanied by formation of a reflected rarefaction wave, and in the second case, the reflected discontinuity is a shock.

The curves of $M_{F_1}(\gamma)$ and $M_{F_2}(\gamma)$ are given in Fig. 3 (curves 1 and 2). Previously, they were obtained in solution of the problem of the interaction of weak perturbations with a shock [7] and in analysis of the properties of isomachs on the plane of ($\beta$, $\Lambda$) [4].

With increase in $J_1$, the position of point 1 relative to curve III (see Fig. 2) depends greatly not only on the values of M and $\gamma$ but also on the intensity $J_1$ of the centered compression wave.

**3.** The analysis of isomachs in Sec. 2 and results of numerical solution of the decay system (1.6) and (1.7) show that for $M < M_{F_1}$, the isomach I of the compression wave is entirely located inside the heart-shaped curve III, and for any value $J_1 \in [1, J_*(M)]$, the reflected discontinuity 2 is a centered rarefaction wave (see Fig. 1b). In this range, the decay system has the form

$$J_3 = J_1 J_2, \quad \omega(M) - 2\omega(M_1) + \omega(M_2) = \beta^{(j)}(M, J_3), \quad \left(\frac{\mu}{\mu_1}\right)^{\eta} = J_1, \quad \left(\frac{\mu}{\mu_2}\right)^{\eta} = J_3. \tag{3.1}$$

Here $M_2$ is the Mach number behind the reflected rarefaction wave 2.

For $M_{F_1} < M < M_s$, the lower portion of the isomach I, which corresponds to the range of intensities of the compression wave $J_1 \in [1, J_{g1}]$, is located outside of the heart-shaped curve III (Fig. 2b). In this range of $J_1$, the reflected discontinuity is a shock (Fig. 1a). For these $J_1$, system (1.6) and (1.7) has the form

$$J_3 = J_1 J_2, \quad \left(\frac{\mu}{\mu_1}\right)^{\eta} = J_1, \quad \omega(M) - \omega(M_1) - \beta^{(j)}(M_1, J_2) = \beta^{(j)}(M, J_3). \tag{3.2}$$

For $J_1 = J_{g1}(M)$, the compression wave decays without reflection (Fig. 1c), and in the range $J_1 \in [J_{g1}, J_*]$, a reflected rarefaction wave occurs again. To determine $J_{g1}$ in formulas (3.1) or (3.2), one should set $J_2 = 1$. This leads to the following system of equations for $J_{g1}$ and $\beta_{g1}$:

$$\omega(M) - \omega(M_1) = \beta^{(j)}(M, J_{g1}), \qquad \mu_1 = \mu J_{g1}^{-1/\eta}. \tag{3.3}$$

The functions $\beta_*(M)$ and $\beta_{g1}(M)$ (curves 1 and 2 in Fig. 4) have a point of tangency for $M = M_s$. At this point, we have $M_1 = M_2 = 1$, $J_2 = 1$, $\omega(M_1) = \omega(M_2) = 0$, and, hence, relation (3.2) leads to the

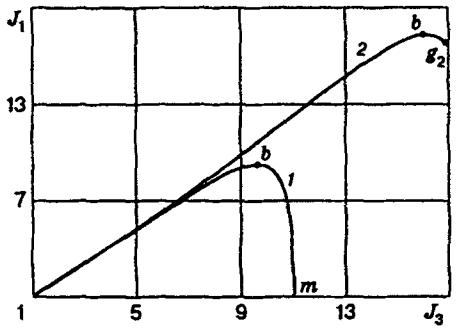


Fig. 5

following equation for $M_s$:

$$\omega(M) = \beta^{(j)}(M, J_3), \qquad J_3 = \mu^{\eta}. \tag{3.4}$$

The curve of $M_s(\gamma)$ is given in Fig. 3 (curve 3).

Thus, in the range of Mach numbers $M \in [M_{F_1}, M_s]$, the reflected discontinuity is a shock for $J_1 \in [1, J_{g1}]$ (region 2 in Fig. 4), and a rarefaction wave for $J_1 \in [J_{g1}, J_*]$ (region $O_1$). Curve 2, which separates the regions $O_1$ and $O_2$ corresponds to decay of the compression wave without reflection.

For $M \in [M_s, M_d]$, the isomach of the compression wave is located outside of the heart-shaped curve III (see Fig. 2c). Hence, the reflected discontinuity can be a shock only. With increase in $J_1$, the dimensions of the heart-shaped curve II, which corresponds to the reflected shock, decrease, and for $J_1 > J_b$, curves II and III do not have points in common. This means that for $M > M_s$ and $J_1 > J_b$, the dynamic-compatibility conditions (1.6) and (1.7) for the tangential discontinuity 4 do not hold. The region $O_3$, bounded by curves 1 and 3 in Fig. 4, corresponds to the parameter values for which system (3.2) does not have solutions.

The position of the boundary of region $O_3$ depends on the behavior of the function $J_1(J_3)$ given by system (3.2). As can be seen from Fig. 2c, for the Mach numbers considered, any intensity $J_1 < J_b$ corresponds to two points of intersection of curves II and III; for $J_1 = J_b$, these points merge into one.

For a fixed Mach number, the curve of $J_1(J_3)$ is nonmonotonic (curve 1 in Fig. 5), and the maximum of the function $J_1(J_3)$ determines the limiting value of the compression-wave intensity $J_b(M)$, beginning from which the problem of wave decay does not have solutions.

Since in (3.2), the relationship between $J_1$ and $J_3$ is implicit, it is reasonable to use the Lagrange method of indefinite multipliers to find the intensities $J_b$. The Lagrange function $F = J_1 + \lambda[\omega(M) - \omega(M_1(J_1)) - \beta_2^{(j)}(M_1(J_1), J_3/J_1) - \beta_3^{(j)}(M, J_3)]$ for fixed M depends only on $J_1$, $J_3$, and $\lambda$ ($\lambda$ is the Lagrange multiplier), because $M_1$ is expressed explicitly in terms of the intensity $J_1$ of this wave [formula (1.4)].

Differentiating $F$ with respect to the indicated variables and setting the resulting expressions to zero, it is not difficult to obtain the following system of equations for $J_b$:

$$\omega(M) - \omega(M_1) - \beta_2^{(j)}(M_1, J_2) = \beta_3^{(j)}(M, J_3); \tag{3.5}$$

$$\frac{\partial \beta_2^{(j)}(M_1, J_2)}{\partial \Lambda_2} + \frac{\partial \beta_3^{(j)}(M, J_3)}{\partial \Lambda_3} = 0, \quad J_1 J_2 = J_3, \quad \mu = \mu_1 J_1^{1/\eta}. \tag{3.6}$$

The derivatives in (3.6) are obtained by differentiating (1.9) with respect to $J$:

$$\frac{\partial \beta^{(j)}}{\partial \Lambda} = \frac{1}{2\gamma J}\sqrt{\frac{\varepsilon}{\chi(J+\varepsilon)}}\,\frac{\delta + \chi(1+\varepsilon)}{\mu(J+\varepsilon) - J(1+\varepsilon J)(1-\varepsilon)},$$
$$\chi = \mu(1+\varepsilon) - (1+\varepsilon J), \quad \delta = \chi(J+\varepsilon) - \varepsilon(1+\varepsilon J)(J-1). \tag{3.7}$$

Now, knowing $J_b(M)$, it is easy to construct a curve of $\beta_b(M)$ (curve 3 in Fig. 4) that corresponds to the boundary of region $O_3$ in which the problem does not have solutions.

For a Mach number $M_d$, the isomachs of the compression wave I and the shocks III have tangency at point $d$ (Fig. 2d). For $M > M_d$, they have two points of intersection: $g_2$ and $g_3$ (Fig. 2e). In the range $J_1 \in [J_{g3}, J_{g2}]$, a portion of the isomach I is located inside the heart-shaped curve III. Hence, for $M > M_d$ again, as for small Mach numbers, there is region $O_4$ in which reflection occurs as a rarefaction wave appears.

The values of $J_d(\gamma)$ and $M_d(\gamma)$ are obtained form the conditions

$$\beta_1^{(i)}(M_d, J_d) = \beta_3^{(j)}(M_d, J_d), \quad \frac{\partial \beta_1^{(i)}(M_d, J_d)}{\partial \Lambda_d} = \frac{\partial \beta_3^{(j)}(M_d, J_d)}{\partial \Lambda_d}. \tag{3.8}$$

The derivative on the right side of (3.8) is determined from formula (3.7), and the derivative on the left side is calculated from $M_1$:

$$\frac{\partial \beta^{(i)}}{\partial \Lambda} = \frac{\sqrt{M_1^2 - 1}}{\gamma M_1^2}. \tag{3.9}$$

The curve of $M_d(\gamma)$ is given in Fig. 3 (curves 4).

The compression-wave intensities $J_{g2}$ and $J_{g3}$ for which the wave decays without reflection are determined by solution of Eq. (3.3); in this case, the intensity $J_{g2}$ should be sought in the range $[J_d, J_b(M)]$ and the values of $J_{g3}$ in the range $[1, J_d]$.

The value $J_{g3} = 1$ occurs for $M = M_{F_2}$ (2.1) and corresponds to the angle $\beta_{g3} = 0$. This means that the point $g_3$ exists only in a narrow range of Mach numbers $M \in [M_d, M_{F_2}]$, descending down the heart-shaped curve III to the coordinate origin with increase in M (Fig. 2f).

The second point of intersection of the isomachs I and II (the point $g_2$) ascends curve I with increase in M and approaches the point $b$, which corresponds to the boundary of the region of absence of solutions (Fig. 2g). For $M = M_b$, the points $b$ and $g_2$ merge (Fig. 2h). As a result, for $M > M_b$, the reflected discontinuity can be a rarefaction wave only (Fig. 2i).

The behavior of the isomachs in the plane of the wave intensities leads to narrowing of the region $O_2$, in which the wave decay is accompanied by a reflected shock. For $M = M_b$, this region disappears. The value of $M_b$ is determined from system (3.5) and (3.6) in which one should set $J_2 = 1$ (curve 5 in Fig. 3).

As can be seen from Fig. 2i, for $M > M_b$, the point $g_2$ does not disappear but its physical meaning changes. Indeed, in the range of intensities $J_1 \in [1, J_{g2}]$, a solution of system (3.1) exists and is unique. However, beginning with the point $g_2$, two points of intersection of curves II and III (points 2a and 2b) correspond to the intensity $J_1$. This situation is typical of the interference theory of shock waves [4]. Usually, in such cases, of two solutions one chose the solution that corresponds to the weaker shock (point 2a).

For $M > M_b$, the type of reflected discontinuity at the point $b$ corresponding to the absence of solution also changes. Accordingly, the system of equations for determining the dependence $J_b(M)$ changes.

To define a system of equations that is similar to (3.5) and (3.6), it is necessary to examine the behavior of the function $J_1(J_3)$ given by Eqs. (3.1). As in the case of a shock, this function is nonmonotonic (curve 2 in Fig. 5), and the maximum point corresponds to the boundary of absence of solution. A test of the function $J_1(J_3)$ for extremum leads to the following system of equations for determining the dependence $J_b(M)$ in the case $M > M_b$:

$$\omega(M) - 2\omega(M_1) + \omega(M_2) = \beta_3^{(j)}(M, J_3); \tag{3.10}$$

$$\frac{\partial \beta_2^{(i)}(M_1, J_2)}{\partial \Lambda_2} + \frac{\partial \beta_3^{(j)}(M, J_3)}{\partial \Lambda_3} = 0, \quad J_1 J_2 = J_3, \quad \mu = \mu_1 J_1^{1/\eta}, \quad \mu_2 = \mu J_3^{-1/\eta}. \tag{3.11}$$

The derivatives in (3.10) and (3.11) are calculated from formulas (3.7) and (3.9) for $j$ and I, respectively.

With a further increase in the Mach number, the scheme of compression-wave decay does not change radically.

4. The value of $\gamma$ has a significant effect on the singular Mach numbers, and, hence, on the boundaries of the characteristic regions of the problem.

Since the value of $M_s$ (3.4) practically does not depend on $\gamma$ (curve 3 in Fig. 3), and over the entire

range $\gamma \in (1.2]$, it is equal to 1.50 with accuracy to the second decimal place, the beginning of the region of absence of solution of the problem depends only slightly on $\gamma$.

In contrast to the weakly decreasing monotonic curve of $M_{F_1}(\gamma)$ (curve 1 in Fig. 3), the function $M_{F_2}(\gamma)$ (curve 2) tends to infinity as $\gamma \to 5/3$. In the range $\gamma \in [5/3.2]$, the reflected discontinuity can be both a rarefaction wave and a shock for any $M > M_d$.

In turn, the function $M_d(\gamma)$ (curve 4 in Fig. 3) exists only for $\gamma \in [1.15; 2]$. For $\gamma < 1.15$, isomachs I and III in Fig. 2 have not more than one point of intersection for any Mach numbers.

Curve 5 in Fig. 3 corresponds to the function $M_b(\gamma)$. Obviously, with increase in $\gamma$ the Mach number $M = M_b$ increases monotonically, reaching the largest value $M_b = 6.844$ for $\gamma = 2$. Hence, there are no significant differences in the behavior of $M_b$ for different $\gamma$.

Analysis of Fig. 2 shows that for small Mach numbers (Fig. 2a and b), the boundary point of isomach I marked by the asterisk and described by formulas (1.5) is located below the top of the heart-shaped curve III. With increase in M, compression-wave intensities for which the static pressure behind the compression wave exceeds the static pressure behind the normal shock appear (Fig. 2c–i). Hence, there is a singular Mach number $M = M_m$ for which the equality $J_* = J_m$ holds; the value of $M_m$ is obtained as a root of the equation

$$\varepsilon \mu_m^{\eta} - (1 + \varepsilon)\mu_m + 1 = 0. \tag{4.1}$$

An analytical solution of Eq. (4.1) exists if $\eta = N + 1$, where $N = 1, 2, 3$. We have $M_m = 2.646$ for $N = 1$ ($\gamma = 2$) and $M_m = 2.226$ for $N = 2$ ($\gamma = 3/2$). For $N = 3$ ($\gamma = 4/3$), Eq. (4.1) is cubic and has a root $M_m = 2.102$. Numerical solution of (4.1) for $\gamma = 1.4$ gives $M_m = 2.151$.

**5.** The maximum flow deflection angle $\beta_m^{(i)}$ in the centered compression wave ignoring the shock-wave interaction at the singular point of the centered wave is obtained from relations (3.1) and (3.2) in which one should set $M \to \infty$:

$$\beta_m^{(i)} = \frac{\pi}{2} \frac{1 - \sqrt{\varepsilon}}{\sqrt{\varepsilon}} \tag{5.1}$$

[$\beta_m^{(i)} = 130.45°$ for $\gamma = 1.4$].

The indicated angle exceeds severalfold the maximum flow deflection angle at the shock $\beta_m^{(j)}$ [4]:

$$\beta_m^{(j)} = \arctan \frac{1 - \varepsilon}{2\sqrt{\varepsilon}} \tag{5.2}$$

[$\beta_m^{(j)} = 45.58°$ for $\gamma = 1.4$]. In addition, the value of $\beta_m^{(i)}$ increases infinitely with decrease in $\gamma$, and this contradicts the physical sense of the problem.

Allowance for the shock-wave interaction at the singular point of the wave imposes a significant restriction on $\beta_m^{(i)}$ in the isentropic compression wave: the limiting angle is defined as the maximum of the function $\beta_b(M)$ which is attained for $M = M_a$ (the point $a$ on curve 3 in Fig. 4). The singular Mach number $M_a$ is determined from analysis of the function $\beta_b(M)$ for extremum and depends only on $\gamma$. From Fig. 3 (curve 6) it is evident that for any angles $\gamma$, the value of $M_a$ is finite, i.e., $\beta_b(\infty) < \beta_b(M_a)$. In this case, in the range $\gamma \in (1, 1.82]$, the maximum of the angle $\beta_b(M)$ corresponds to a reflected rarefaction wave ($M_a > M_b$), and for $\gamma \in [1.82, 2]$, the maximum flow deflection angle occurs in the system with a reflected shock.

The calculations performed show that, in contrast to the angle $\beta_m^{(i)}$ (5.1), the angle $\beta_a = \beta_b(M_a)$ is finite for any $\gamma \in (1, 2]$: the function $\beta_a(\gamma)$ decreases monotonically from $\beta_a = 53.135°$ ($\gamma \to 1$) to $\beta_a = 28.308°$ ($\gamma = 2$). In addition, for any $\gamma$, the angle $\beta_a$ is lower than the maximum flow deflection angle $\beta_m^{(j)}$ (5.2) at the shock.

Furthermore, it should be noted that the maximum overall flow deflection angle in the system, which coincides with the maximum flow deflection angle at the resulting shock 3 (see Fig. 1), increases monotonically with increase in M and tends to $\beta_m^{(j)}$ (5.2) as $M \to \infty$.

**6.** As shown in [5, 6], an isentropic compression wave is used to produce optimal shock-wave systems.

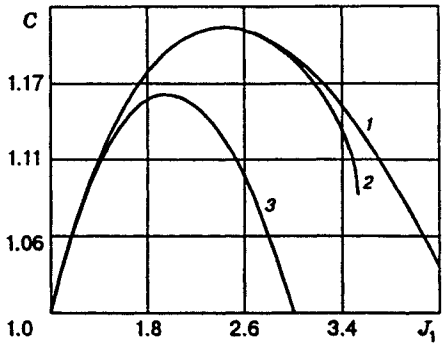


Fig. 6

In practice, the gas-dynamic design of such systems is implemented in such a manner that the wave is centered [5], and the flow past the wave does not show extremal properties.

An important and most common problem of controlling a supersonic flow is to decelerate the flow to subsonic velocities with minimum losses of total pressure. An obvious solution of this problem involves the generation of an isentropic compression wave with intensity $J_*(M)$ (1.5), which decelerates the flow to the velocity of sound. However, allowance for the wave decay at the singular point shows that for any Mach numbers, the flow behind the reflected discontinuity 2 (see Fig. 1) is supersonic for all intensities of the isentropic wave in the range of existence of solutions.

Indeed, in the range $M \in [1, M_s]$, a supersonic flow that decelerates to the sound velocity in a compression wave of intensity $J_*$ accelerates again in the reflected rarefaction wave. When $M > M_s$, the intensity $J_*$ is in the region $O_3$ in which the problem does not have solutions (see Fig. 4). Behind waves whose intensities are in the range $[1, J_b]$ in which a solution of the problem exists, the flow is supersonic both behind the wave and the reflected discontinuity. Hence, a solitary centered compression wave cannot decelerate the flow to subsonic velocity. Therefore, to solve the formulated problem, it is necessary to use optimal systems that consist of shocks only [6] or to produce an additional subsonic shock behind an isentropic wave.

It has been proved [6] that for $M > \sqrt{2}$, an isentropic compression wave can be used to advantage for maximum recovery of the velocity head. Figure 6 gives the ratio of the velocity head ahead of and behind the wave (curve 1, constructed for $M = 2$), calculated from the formula [1]

$$C \equiv \frac{\rho_1 v_1^2}{\rho v^2} = \frac{\mu J_1^{1/\gamma} - (1-\varepsilon)J_1}{\mu - (1-\varepsilon)}.$$

It can be seen from Fig. 6 that the function $C(J_1)$ reaches a maximum for $J_1 = J_g$:

$$J_g = \left(\frac{\mu}{1+\varepsilon}\right)^{\eta}.$$

Hence, an isentropic wave with intensity $J_g$ is an optimal wave for the velocity head.

The calculations performed show that allowance for the interaction at the singular point in the range $M \in [\sqrt{2}, 2.6]$ practically does not affect the position of the maximum (curve 2 in Fig. 6). However, with increase in M, the intensity corresponding to the maximum gradually approaches the boundary of the region in which solutions are absent, and for $M > 2.6$, it disappears. As a result, for large values of M, the ratio of the velocity heads increases monotonically with increase in $J$ and reaches a maximum for $J = J_b$, i.e., on the boundary of the region in which solutions are absent.

In contrast to the ratio of the velocity heads in the regions below the tangential discontinuity, the ratio of the velocity heads at the resulting shock behaves nonmonotonically for any values of M (curve 3 in Fig. 6), reaching a maximum for a certain intensity $J_d$ of the compression wave. Calculations show that this quantity can be approximated with high accuracy by the expression of the intensity of a solitary shock that is optimal

for the velocity head [6]:

$$J_d \approx (\sqrt{\mu(1+\varepsilon)} - 1)/\varepsilon.$$

The results obtained suggest that a centered compression wave with intensity $J_1 = J_d$ can be used for recovery of the velocity head. For this intensity, the velocity head is high both above and below the tangential discontinuity. A further increase in $J_1$ facilitates growth of the examined function behind the reflected shock 2 (see Fig. 1). Simultaneously this leads to an increase in the velocity head behind the shock 3, making worse the integral characteristics of the velocity head in the flow behind the point of discontinuity decay.

This work was supported by the Foundation for Research in Fundamental Natural Sciences (Grant No. 95-0-4.2-171)

## REFERENCES

1. L. D. Landau and E. M. Lifshits, *Hydrodynamics* [in Russian], Nauka, Moscow (1988).
2. G. S. Roslyakov, "Interaction of plane unidirectional shocks," in: *Numerical Methods in Gas Dynamics* [in Russian], Izd. Moscow Univ., Moscow (1965), pp. 28–51.
3. G. S. Roslyakov, A. L. Starykh, and V. N. Uskov, "Interference of stationary unidirectional shocks," *Izv. Akad. Nauk SSSR, Mekh. Zhidk. Gaza*, No. 4, 143–152 (1985).
4. A. L. Adrianov, A. L. Starykh, and V. N. Uskov, *Interference of Stationary Gas-Dynamic Discontinuities*, Nauka, Novosibirsk (1995).
5. V. I. Kireev and A. S. Voinovskii, *Numerical Modeling of Gas-Dynamic Flows* [in Russian], Izd. Mosk. Aviats. Inst., Moscow (1991).
6. A. V. Omel'chenko and V. N. Uskov, "Optimal shock-wave systems," *Izv. Ross. Akad. Nauk, Mekh. Zhidk. Gaza*, No. 6, 118–126 (1995).
7. G. G. Chernyi, *High Supersonic Velocity Gas Flows* [in Russian], Fizmatgiz, Moscow (1959).